

X-ray scattering by highly polished surfaces

A. V. Vinogradov, N. N. Zorev, I. V. Kozhevnikov, S. I. Sagitov, and A. G. Tur'yanskiĭ

P. N. Lebedev Physics Institute, Academy of Sciences of the USSR, Moscow

(Submitted 7 July 1987)

Zh. Eksp. Teor. Fiz. **94**, 203–216 (August 1988)

The scattering function for x radiation reflected from a surface with an extremely slight roughness is analyzed in the Andronov-Leontovich model. Several features of the scattering function and of the integral scattering are described quantitatively in two intervals of the glancing angle θ_0 of the incident radiation: $\theta_0 < \theta_c$ and $\theta_0 > \theta_c$, where θ_c is the critical angle for total external reflection. Among these features are a broadening and a shift of the peak of the scattered radiation, the appearance of additional peaks on the function, and an apparent increase in the height of the surface roughness, which is observed at small glancing angles. The scattering function of CuK_α radiation during reflection from samples of various materials has been measured.

INTRODUCTION

In 1913 Mandelstam¹ examined several physical questions concerning the observation of molecular motions of a free liquid surface by optical methods. Andronov and Leontovich² subsequently analyzed the electrodynamic part of the problem and actually laid the foundation for a description of the scattering which arises in many phenomena in the reflection of radio waves from the earth's surface,^{3,4} in the reflection of slow neutrons from solids,⁵ in the reflection of visible light from optical surfaces,^{6–8} and in the reflection of sound waves from interfaces.^{9,10} It should be noted, however, that Andronov and Leontovich's paper² is not well known, and its results have been repeatedly rederived by various investigators.

Scattering methods have recently acquired new importance because of technological advances in x-ray and neutron research. Cold neutrons with an energy of $2 \cdot 10^{-3}$ – $2 \cdot 10^{-5}$ eV and x rays with an energy of 1–10 keV have a wavelength $\lambda \sim 1$ – 10 \AA ; these wavelengths correspond to estimates of the minimum dimensions of surface defects and of surface roughness. Accordingly, a significant scattering should arise in this wavelength region even when absolutely the best methods are used to prepare surfaces. This circumstance would be extremely convenient for observing scattering and for studying ultrasoft surfaces on the basis of this scattering. In addition, scattering by surface roughness is one of the most important factors limiting the quality and potential application of x-ray optics and neutron optics, which are of interest in a long list of scientific and technological fields.

Experimental research on the scattering during the reflection of x radiation from various materials is being carried out in connection with problems in x-ray astronomy, plasma diagnostics, x-ray microscopy and spectroscopy, microlithography, etc. It has been shown^{11–15} that two features can be observed in the scattering of x radiation incident at grazing angles on an interface.

1. The height of the roughness at the interface calculated from the total integral scattering increases with decreasing glancing angle.^{11,12} This behavior contradicts most of the theoretical models which are presently in use; these models lead to the familiar expression^{16,17}

$$I = I_0 \left\{ 1 - \exp \left[- \left(\frac{4\pi\zeta}{\lambda} \sin \theta_0 \right)^2 \right] \right\} \\ \approx I_0 \left(\frac{4\pi\zeta}{\lambda} \sin \theta_0 \right)^2, \quad \frac{\zeta \sin \theta_0}{\lambda} \ll 1,$$

where I and I_0 are the scattering intensity and the intensity of the incident radiation, respectively, λ is the wavelength, ζ is the roughness height, and θ_0 is the glancing angle of the incident radiation.

2. If the glancing angle of the incident radiation, θ_0 , is greater than θ_c , which is the critical angle for total external reflection, the scattering function will have two peaks: one in the specular reflection direction and another at an angle from the surface close to the critical angle.^{13–15}

We wish to stress that both of these effects are seen at small glancing angles, where the x-ray reflection coefficient is large. These effects are thus of interest not only for research on surfaces but also for reflection grazing-incidence x-ray optics, which is finding progressively wider use in fundamental and applied physics. Since diffuse-scattering methods are of practical importance in x-ray optics and surface physics, it is extremely desirable to find a quantitative explanation for both of these effects.

In the present paper we show that both of these effects can be described by the methods of Andronov and Leontovich,² i.e., through the systematic application of perturbation theory to a simple and graphic model of a surface.

In Sec. I we present the basic equations describing the surface model and the interaction of a monochromatic plane wave with the surface. We present these equations without derivation, following Refs. 2, 18, and 19. We give a relation between the scattering function and the correlation function of an isotropic surface. We discuss the use of this relation in measurements of the correlation function. This relation serves as a starting point for the sections of the paper which follow. A necessary condition for the applicability of this relation is that the perturbation theory be valid. The accuracy of the perturbation theory improves with improvements in the quality of the surface finish, as was demonstrated convincingly even in the early papers by Leontovich.^{2,6}

In Sec. II we examine the shape of the x-ray scattering function. Some conditions arise here which simplify the

analysis: $\lambda \ll a$, $\theta_0 \lesssim \theta_c \ll 1$, where a is the correlation radius of the roughness heights. As a result, it becomes appropriate to deal with the scattering function integrated over φ , i.e., $\pi(\theta)$, instead of the doubly differential scattering function $\Phi(\theta, \varphi)$ (θ and φ are the angles specifying the scattering direction). This comment applies to both experimental and theoretical research. This integral scattering function takes different forms in four regions defined by the magnitudes of and relations between the parameters $\mu = \pi a \theta_0^2 / \lambda$ and $\mu_c = \pi a \theta_c^2 / \lambda$. In particular, in the region $\mu_c > \mu \gg 1$ there is an analogy with the optical range, where the scattering function is bell-shaped with a diffractive width $\Delta\theta \sim \lambda / a \theta_0$. Another interesting case is the Yoneda effect,¹³ which was discussed in Refs. 14, 15, and 20. The Yoneda effect is manifested if the glancing angle of the incident radiation, θ_0 , exceeds the critical angle for total external reflection, θ_c (i.e., $\mu > \mu_c$). It consists of the appearance of an additional maximum in the scattering function. Finally, one should distinguish two other intervals of the parameters μ and μ_c ($\mu \ll 1$, $\mu_c \gg 1$ and $\mu < \mu_c \ll 1$), in which the scattering function has a characteristic shape, and its width does not depend on the glancing angle.

In Sec. III we examine the integral intensity of the scattered radiation for conditions corresponding to the x-ray range. It is this intensity which is used to measure the height of surface roughness by the total-integral-scattering method. Analysis of the consequences of the rigorous scattering theory shows that the dependence of the integral scattering intensity on the glancing angle changes in nature when we switch from large glancing angles ($\mu \gg 1$) to small glancing angles ($\mu \ll 1$). This circumstance makes it possible to explain the experimental results of Refs. 11 and 12 and to establish a range of applicability for the total-integral-scattering method.

I. GENERAL RELATIONS

Scattering function. Let us assume that the interface between the material (which has a dielectric constant ε) and the vacuum is described by the equation $z = \zeta(\rho)$, where ζ is a random function which determines the statistical properties of the surface, the $z = 0$ plane corresponds to the position of the ideally smooth interface (i.e., $\langle \zeta(\rho) \rangle = 0$), and the vector ρ lies in the xy plane (Fig. 1). We assume that the properties of the material change abruptly at the interface. The spatial distribution of the dielectric constant can then be written in the form

$$\varepsilon(\mathbf{r}) = \varepsilon_0(z) + \Delta\varepsilon(\mathbf{r}), \quad \varepsilon_0(z) = 1 - (1 - \varepsilon)H(z), \\ \Delta\varepsilon(\mathbf{r}) = (1 - \varepsilon)[H(z) - H(z - \zeta(\rho))], \quad \mathbf{r} = (\rho, z),$$

where H is the (Heaviside) unit step function: $H(z) = 0$ at $z < 0$ and $H(z) = 1$ at $z > 0$.

The reflection and scattering of the radiation by a rough surface are described in the scalar approximation by the equation

$$[\nabla^2 + k^2 \varepsilon_0(z)] \Psi(\mathbf{r}) = -k^2 \Delta\varepsilon(\mathbf{r}) \Psi(\mathbf{r}),$$

where $k = \omega/c = 2\pi/\lambda$ is the wave number in vacuum, and $\Psi(\mathbf{r})$ is the wave amplitude. With ultrasurface in mind, we will use a perturbation theory in the roughness height ζ (Refs. 2 and 19). The integral intensity of the scattered radiation can then be written in the form¹⁹

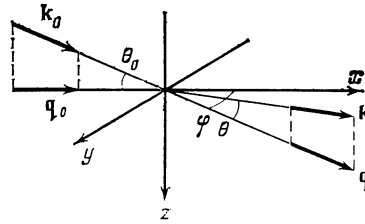


FIG. 1. Diagram illustrating the reflection of x radiation from a rough interface between two media. k_0, k —Wave vectors of the incident and scattered radiation; q_0, q —projections of these vectors onto the xy plane.

$$I = I_0 \int_0^{\pi/2} \cos \theta \, d\theta \int_0^{2\pi} \Phi(\theta, \varphi) \, d\varphi, \quad (1)$$

where $\Phi(\theta, \varphi)$ is the scattering function, given by

$$\Phi(\theta, \varphi) = \frac{1}{I_0} \frac{dI}{d\Omega} = \frac{2k^4}{\pi} R(\theta_0) \frac{T(\theta)}{T(\theta_0)} \chi_F(\mathbf{q} - \mathbf{q}_0) \sin^3 \theta, \\ \chi_F(\mathbf{q} - \mathbf{q}_0) = \frac{1}{2\pi} \int d^2\rho \exp[i(\mathbf{q} - \mathbf{q}_0)\rho] \chi(\rho), \quad (2)$$

$$T(\theta) = \frac{4 \sin^2 \theta}{|\sin \theta + (\varepsilon - \cos^2 \theta)^{1/2}|^2},$$

$$R(\theta) = \left| \frac{\sin \theta - (\varepsilon - \cos^2 \theta)^{1/2}}{\sin \theta + (\varepsilon - \cos^2 \theta)^{1/2}} \right|^2.$$

Here $R(\theta)$ is the reflection coefficient, and the quantity $T(\theta) \text{Re}[(\varepsilon - \cos^2 \theta)^{1/2} / \sin \theta]$ is the transmission coefficient of the ideally smooth interface for a wave. The angles θ , φ , and θ_0 which appear in the expression (2) are shown in Fig. 1; q_0 and q are the projections of the wave vectors of the incident and scattered radiation onto the xy plane; $\chi(\rho) = \langle \zeta(\mathbf{r}) \zeta(\mathbf{r} + \rho) \rangle$ is the correlation function of the roughness heights; and, in particular, $\chi(0) = \langle \zeta^2 \rangle$ is the mean square roughness height (below, we will omit the symbol indicating an average).

We wish to stress that the scattering function (2) depends not only on the statistical properties of the interface [i.e., the correlation function $\chi(\rho)$] but also on parameters which are unrelated to the microscopic geometry of the surface: the wavelength λ , the glancing angle of the incident radiation, θ_0 , and the dielectric constant of the material, ε . As these parameters are varied, the shape of the scattering function may vary in an extremely complicated way.

In addition to the scattered radiation, the beam reflected by a surface contains a specular component, whose angular distribution reproduces that of the incident beam. The specular component is less informative than the scattering function for research on surfaces, but it is an important characteristic of any optical element. The specular component was studied in Ref. 19 for the case of the reflection of x radiation from a rough surface.

Isotropic surfaces. In this case the correlation function of the roughness heights depends on a single variable: $\chi(\rho) = \chi(|\rho|)$. The scattering function (2) takes the form

$$\Phi(\theta, \varphi) = \frac{2k^4}{\pi} R(\theta_0) \frac{T(\theta)}{T(\theta_0)} \chi_B(\nu) \sin^3 \theta_0,$$

$$\chi_B(\nu) = \int_0^\infty \rho \chi(\rho) J_0(\nu \rho) d\rho, \quad (3)$$

$$\nu = |\mathbf{q} - \mathbf{q}_0| = k(\cos^2 \theta + \cos^2 \theta_0 - 2 \cos \theta \cos \theta_0 \cos \varphi)^{1/2},$$

where $J_0(x)$ is the Bessel function. Expressions (3) show that it is a simple matter to work from the measured scattering function $\Phi(\theta, \varphi)$ to determine the function $\chi_B(\nu)$, which is related to the correlation function $\chi(\rho)$ by a Bessel transformation. If the dielectric constant of the material, $\varepsilon(\omega)$, and thus R and T , according to expression (2), are known quite reliably, then one can measure the correlation function $\chi_B(\nu)$ by probing the surface with radiation at various wavelengths, ranging from the visible range to the x-ray range. The approach improves the reliability of the results considerably. Let us discuss this question in more detail.

If the values of $\chi_B(\nu)$ were known for all values of the parameter $\nu \in [0, \infty]$, the correlation function $\chi(\rho)$ would be determined by the inverse transformation:

$$\chi(\rho) = \int_0^\infty \nu \chi_B(\nu) J_0(\nu \rho) d\nu, \quad \xi^2 = \chi(0) = \int_0^\infty \nu \chi_B(\nu) d\nu. \quad (4)$$

In practice, on the other hand, in measurements of the scattering function $\Phi(\theta, \varphi)$ at a fixed wavelength λ the function $\chi_B(\nu)$ can be determined in only a finite interval of values of ν : $\nu_{\min} < \nu < \nu_{\max}$. As can be seen from expressions (3), as the angles θ_0 , θ , and φ are varied, but the wavelength of the incident radiation, λ , is held fixed, the values of ν cannot exceed $\nu_{\max} = 2k = 4\pi/\lambda$. From this result follows, in particular, the obvious fact that the microscopic geometry of the surface can be determined progressively more accurately as the wavelength λ of the probing radiation becomes shorter. The minimum transverse dimensions of the surface irregularities that can be detected are of order $a_{\min} \sim \nu_{\max}^{-1} \approx \lambda/4\pi$. The value of ν is bounded below by the finite angular spread $\delta\theta$ of the incident radiation, since in the range of angles θ between $\theta_0 - \delta\theta/2$ and $\theta_0 + \delta\theta/2$ it is impossible in practice to distinguish the scattered radiation from the specularly reflected beam. From this it follows that

$$\nu_{\min} \approx \frac{1}{2} k \delta\theta \sin \theta_0, \quad \alpha_{\max} \sim \nu_{\min}^{-1} \approx (\lambda/\pi) \delta\theta \sin \theta_0.$$

Hence the correlation function $\chi(\rho)$ of the height of the surface roughness can be determined from the scattering index, strictly speaking, only for a beam of zero divergence with wavelength λ taken to zero.

In practice it is quite unnecessary to know the correlation function $\chi(\rho)$ for many applications. The function $\chi_B(\nu)$ on some interval $\nu \in [\nu_1, \nu_2]$ determined by the experimental conditions contains all the requisite information. In particular, this is the case when the surface optical properties in some spectral range are being investigated. Hence the most natural approach is to use Eqs. (3) to determine $\chi_B(\nu)$ by measuring the scattering index in the required range of ν . For this purpose no *a priori* assumptions are needed regarding the form of $\chi(\rho)$. Moreover, analysis of Eqs. (3) shows that from measurements of $\Phi(\theta, \varphi)$ at some wavelength λ in

some range of θ and φ it is possible in principle to find $\chi_B(\nu)$ and predict the scattering index $\Phi(\theta_1, \varphi_1)$ at some different wavelength λ_1 and angles θ_1 and φ_1 . Doing this will of course require a precise knowledge of the optical constants [which determine $R(\theta)$ and $T(\theta)$ in (3) at both wavelengths, λ and λ_1].

Everything which we said above regarding the relationship between the surface correlation function $\chi_B(\nu)$ and the scattering function which is differential in θ and φ , i.e., $\Phi(\theta, \varphi)$, is valid for arbitrary wavelengths λ and arbitrary glancing angles θ_0 . The choice of a particular wavelength and a particular glancing angle depends on the properties of the surface and the experimental conditions. In the sections of this paper which follow we will examine the particular features of the scattering of x radiation.

II. SCATTERING FUNCTION FOR X RADIATION

Small glancing angles; integration of the scattering function over φ . We first note that in the x-ray range there is no point in considering glancing angles other than small ones, $\theta_0 \lesssim \theta_c \ll 1$, at which the reflection coefficient is not small. We also assume, for simplicity, that the function $\chi_B(\nu)$ reaches a maximum at $\nu = 0$ and falls off monotonically with increasing value of the parameter ν . According to (3), we can then conclude that the scattering function has a maximum near $\nu = 0$, i.e., near the specular component. This assumption seems completely reasonable.

From the explicit expression for ν [see (3)] we find, noting that the angles are small, $\theta_0, \theta, \varphi \ll 1$, that the angular width $\Delta\theta$ of the function $\chi_B(\nu)$ in the plane of incidence (and thus also the angular width of the scattering function) and the angular width $\Delta\varphi$ in the perpendicular direction (along the angle φ) are related by

$$\Delta\varphi \sim \theta_0 \Delta\theta \ll \Delta\theta.$$

Second, the wavelength of x radiation is considerably shorter than the correlation radius, a , which is 0.1–10 μm for most surfaces. For example, if the glancing angle θ_0 and the width of the scattering function in the plane of incidence, $\Delta\theta$, are a few degrees, the width of the scattering function in terms of the angle φ , i.e., $\Delta\varphi$, will be only a matter of arc minutes (see also Ref. 21).

By virtue of these two circumstances, in the x-ray range it turns out to be a particularly simple matter to experimentally determine the scattering function $\Pi(\theta)$ integrated over the angle φ (i.e., over the directions perpendicular to the plane of incidence):

$$\Pi(\theta) = \int \Phi(\theta, \varphi) d\varphi = 4k^4 R(\theta_0) \frac{T(\theta)}{T(\theta_0)} \sin^3 \theta_0 \cdot \int_0^\infty \rho \chi(\rho) J_0(k\rho \cos \theta) J_0(k\rho \cos \theta_0) d\rho. \quad (5)$$

Expression (5) was derived from (3) and is exact. We now use the relation $a \gg \lambda$ and expand the Bessel functions at large values of their argument. We find

$$\Pi(\theta) = \frac{4k^3}{(2\pi)^{1/2}} R(\theta_0) \frac{T(\theta)}{T(\theta_0)} \chi_c(p) \sin^3 \theta_0,$$

$$\chi_c(p) = \left(\frac{2}{\pi}\right)^{1/2} \int_0^\infty \chi(\rho) \cos p\rho d\rho, \quad p = k|\cos \theta - \cos \theta_0|. \quad (6)$$

Consequently, by measuring the scattering function $\Pi(\theta)$ integrated over the angle φ in the x-ray range, we can easily find the function $\chi_c(p)$, which determines only the statistics of the surface, as in the general case, (3). The only difference is that a Bessel transformation of the correlation function $\chi(p)$ appears in the differential scattering function $\Phi(\theta, \varphi)$ [expression (3)], and a Fourier cosine transformation appears in expression (6) for $\Pi(\theta)$. These transformations are related by

$$\chi_c(p) = \left(\frac{2}{\pi}\right)^{1/2} \int_p^\infty dv \chi_s(v) \frac{v}{(v^2 - p^2)^{1/2}}.$$

If the function $\chi_c(p)$ were known for all values of the parameter p , the correlation function could be calculated by taking inverse Fourier transforms:

$$\chi(\rho) = \left(\frac{2}{\pi}\right)^{1/2} \int_0^\infty \chi_c(p) \cos p\rho dp,$$

$$\xi^2 = \chi(0) = \left(\frac{2}{\pi}\right)^{1/2} \int_0^\infty \chi_c(p) dp.$$

Transforming from the differential scattering function $\Phi(\theta, \varphi)$ to the scattering function which is integrated over φ , i.e., $\Pi(\theta)$, may not be correct in the visible range. The reason is that expression (6) holds when the conditions $ka \cos \theta \gg 1$ and $ka \cos \theta_0 \gg 1$ hold, as they do at small glancing angles in the x-ray range, but they do not hold in the visible range, especially at normal incidence.

In moving on to an analysis of the x-ray scattering function, we will distinguish between the region of total external reflection ($\theta_0 < \theta_c$) and the region of the Yoneda effect ($\theta_0 > \theta_c$) (Refs. 13–15).

Scattering function in the region of total external reflection ($\theta_0 < \theta_c$). It can be seen from expression (6) that the shape of the scattering function, i.e., its dependence on the observation angle θ (Fig. 1), is determined by the product of the functions $T(\theta)$ and $\chi_c(p)$, where $p = p(\theta)$. [The entire analysis below is also valid for a scattering function as in (3) in the plane of incidence, i.e., at $\varphi = 0$.] The function $T(\theta)$ is determined exclusively by the optical properties of the material, and the function $\chi_c(p)$ by the statistics of the roughness of the interface. Clearly, if the function $\chi_c(p)$ has features of any sort, they will, in general, be observed in the scattering function. We restrict the analysis to the simplest case, in which $\chi_c(p)$ reaches a maximum at $p = 0$ (i.e., at $\theta = \theta_0$) and falls off monotonically with increasing value of the parameter p . We assume that the scale of the variation in $\chi_c(p)$ is $p \sim a^{-1}$, where a is the correlation radius of the roughness heights. Furthermore, we ignore the absorption of radiation in the material; i.e., we set $\text{Im } \varepsilon = 0$. The function $T(\theta)$ then takes the form

$$T(\theta) = \begin{cases} 4\theta^2/\theta_c^2, & \theta \leq \theta_c = (1-\varepsilon)^{1/2} \\ 4\theta^2[\theta + (\theta^2 - \theta_c^2)^{1/2}]^{-2}, & \theta > \theta_c \end{cases}$$

The value of T reaches a maximum at $\theta = \theta_c$ and falls off rapidly to its asymptotic value as we leave the region of total external reflection: $T(\theta) \rightarrow 1$ at $\theta > \theta_c$.

Let us examine the features of the shape of scattering function $\Pi(\theta)$ as a function of the correlation radius a and the glancing angle of the incident radiation, θ_0 . We assume

that the angle θ_0 lies in the region of total external reflection: $\theta_0 < \theta_c$ (Fig. 2, a and b). We will examine the case $\theta_0 > \theta_c$ below. We introduce the parameters

$$\mu = ka\theta_0^2/2, \quad \mu_c = ka\theta_c^2/2 \quad (7)$$

and we consider three limiting cases.

1. The correlation radii are large, and the glancing angles of the incident radiation, θ_0 , are not too small: $\mu_c \gg 1$ and $\mu \gg 1$ (line 1 in Fig. 2b). The angular position θ_m of the maximum of the scattering function is determined by the following equation for any values of μ and μ_c :

$$-\chi_c(p) \left/ \frac{d\chi_c}{dp} \right. (p) = p + \frac{k\theta_0^2}{2}, \quad p = k(\cos \theta_0 - \cos \theta_m), \quad (8)$$

$$\theta_0 < \theta_c.$$

In the particular case under consideration here, $\mu, \mu_c \gg 1$, the maximum of the scattering function essentially coincides with the specular-reflection direction, as can be seen from an analysis of Eq. (8). The peak has a symmetric shape, and its angular width $\Delta\theta$ is determined exclusively by the width of the function $\chi_c(p)$:

$$\Delta\theta \sim \lambda/\pi a \theta_0, \quad \theta_m \approx \theta_0. \quad (9)$$

2. The correlation radii are large, and the glancing angles of the incident radiation are extremely small $\mu_c \gg 1$ but $\mu \ll 1$ (line 1 in Fig. 2a). From expression (9) we see that the scattering function broadens with decreasing value of the glancing angle θ_0 . If θ_0 becomes so small that the interface begins to intersect the scattering function ($\Delta\theta \sim \lambda/\pi a \theta_0 \sim \theta_0$; i.e., $\mu \sim 1$), we would naturally expect a change in the nature of the scattering.

It can be seen from Eq. (8) that at extremely small values θ_0 (i.e., $\mu \ll 1$) the maximum of the scattered radi-

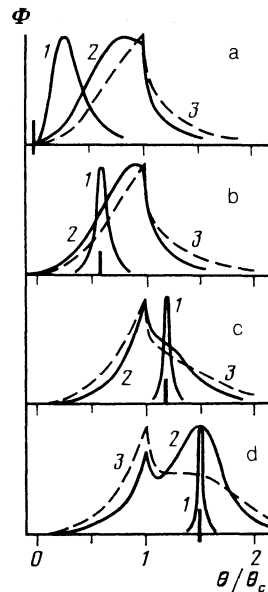


FIG. 2. The shape $\Phi(\theta)$ of the scattering function versus the glancing angle of the incident beam, θ_0 . a— $\theta_0/\theta_c = 0$; b—0.6; c—1.2; d—1.5. The shape versus the correlation radius of the roughness heights, a: 1— $\mu_c = \pi a \theta_0^2/\lambda = 10$; 2—1; 3—0.5. Absorption has been ignored. The correlation function was chosen to be exponential, $\chi(\rho) = \xi^2 \exp(-\rho/a)$, in the calculations. The vertical bars show the position of the specularly reflected beam.

ation shifts with respect to the beam which is reflected specularly from the surface. At the same time, the scattering peak becomes asymmetric, and its angular width becomes

$$\Delta\theta \sim \theta_m \sim (\lambda/\pi a)^{1/2}.$$

3. The correlation radii are small: $\mu_c \ll 1$ (lines 3 in Fig. 2, a and b). In this case the function $\chi_c(p)$ remains essentially constant in the region of total external reflection ($\theta < \theta_c$), and the shape of the scattering function corresponds to the dependence $T(\theta)$. In particular, the maximum of the scattered radiation occurs at the critical angle for total external reflection:

$$\theta_m \approx \theta_c, \quad \Delta\theta \sim \theta_c/2.$$

Case 1 corresponds to the scattering pattern which is ordinarily observed in the visible range. Cases 2 and 3 are specifically characteristic of the x-ray range. Case 2 was observed in Ref. 22 but interpreted there on the basis of a more complicated model of the surface. Case 3—scattering by surfaces with very small correlation radii—is characterized by a scattering-function maximum which lies near the critical angle, regardless of the glancing angle of the incident beam. This effect has not been observed previously in x-ray scattering and has not been discussed.

The Yoneda effect. Let us examine the features which appear in the scattering function in the case in which the glancing angle of the incident radiation, θ_0 , exceeds the critical angle for total external reflection, θ_c . We will show that the simple intuitive model of a surface which was presented above is successful in explaining the anomalous scattering of x radiation (the Yoneda effect) which was observed in Refs. 13–15 (and described theoretically in Refs. 14, 20, and 22 on the basis of more complicated models of an interface and under additional assumptions regarding the structure of the electromagnetic field). Briefly, the effect is the appearance of an additional peak in the scattering function if $\theta_0 > \theta_c$.

We used a BSV-8 x-ray tube with a copper anode in measurements of the scattering function carried out in order to observe the Yoneda effect. A pyrolytic-graphite monochromator selected the characteristic CuK_α line ($\lambda = 1.54 \text{ \AA}$). The angular distribution of the scattering was measured in the plane of incidence of the direct beam. The collection angle, set by the receiving slit of the detector, and the angular divergence of the direct beam in this plane were $1'$ and $2'$, respectively. The angular divergence in the plane perpendicular

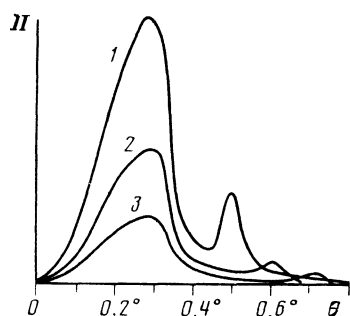


FIG. 3. Experimental angular distribution of the scattering of x radiation ($\lambda = 1.54 \text{ \AA}$) from a tin film $0.4 \mu\text{m}$ thick deposited on a substrate of K8 glass, for various glancing angles of the incident beam: 1— $\theta_0 = 0.5^\circ$; 2— 0.6° ; 3— 0.7° . The critical angle for total external reflection is $\theta_c \approx 0.28^\circ$.

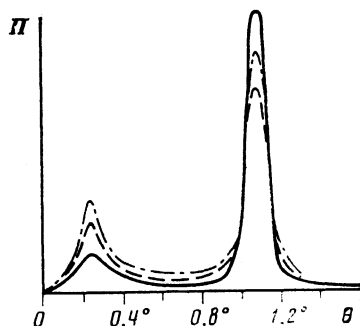


FIG. 4. The same as in Fig. 3, for three different samples of K8 glass and for the glancing angle $\theta_0 = 1^\circ$. The critical angle is $\theta_c \approx 0.22^\circ$.

ular to the plane of incidence was $\sim 1^\circ$, limited by a Soller slit. As samples we used plates of a plastic ($\text{C}_5\text{H}_8\text{O}_2$), K8 glass, and a tin film with a surface with a mirror finish (in the optical range). A tin film $0.4 \mu\text{m}$ thick was vacuum-deposited on a substrate of K8 glass.

Figures 3–5 show angular distributions of the scattering found experimentally (the specular component has not been subtracted). An anomalous-scattering effect was observed for all of the samples studied. This anomalous scattering consisted of the appearance of an additional peak on the scattering distribution at observation angles $\theta \approx \theta_c$. The position of this peak depended weakly on the glancing angle of the incident beam, θ_0 , as θ_0 was varied from $1.8\theta_c$ to $2.6\theta_c$ (Fig. 3). It also depended weakly on the microscopic geometry of the surface (Fig. 4).

Let us use expression (6) to discuss the results.¹¹ In the first place, it is clear [see (3) and (6)] that the maximum of the function $\chi_c(p)$ at $\theta = \theta_0$ [or the maximum of $\chi_B(\nu)$ $\theta = \theta_0$ and $\varphi = 0$] corresponds to the ordinary scattering peak in the specular direction. Furthermore, in the absence of absorption the function $T(\theta)$ has the following singularity:

$$\frac{dT}{d\theta} (\theta \rightarrow \theta_c + 0) \rightarrow -\infty, \quad \text{Im } \varepsilon = 0.$$

This result means that, regardless of the function $\chi_c(p)$, the intensity of the scattered radiation falls off in a certain interval of observation angles θ lying to the right of the critical angle θ_c . Consequently, if the incident beam lies outside the region of total external reflection ($\theta_0 > \theta_c$), there will be an

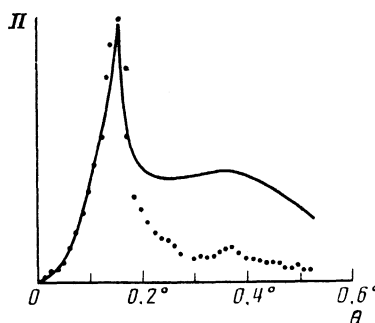


FIG. 5. The same as in Fig. 3, for a plastic sample with a glancing angle $\theta_0 = 0.375^\circ$ (dots); results calculated from expression (6) for an exponential correlation function and a correlation radius $a = 1 \mu\text{m}$ (solid line). The critical angle is $\theta_c \approx 0.16^\circ$.

additional maximum in the scattering function, at an angular position which coincides with the critical angle for total external reflection (an anomalous-scattering peak).

If this peak is to be observed experimentally, there are nevertheless certain conditions which must be satisfied (Fig. 2, c and d, and Fig. 6).

1. There must be a fine-scale roughness with small correlation radii at the surface:

$$\mu_c \ll 1, \quad \text{i.e., } a \ll \lambda / \pi \theta_c^2. \quad (10)$$

Otherwise, the rapid decrease in the function $\chi_c [p(\theta)]$ away from the specular-reflection direction will have the consequence that even if the glancing angle θ_0 differs only slightly from θ_c the height of the anomalous-scattering peak will become exceedingly small. At the scale of Fig. 2d, for example, this peak is simply not seen on line 1.

2. For a reliable separation of two peaks in the scattered radiation, we would like to keep the glancing angle θ_0 fairly far from the critical angle θ_c . On the other hand, θ_0 must not be too large, for otherwise the height of the anomalous-scattering peak will become too small because of the finite angular width of the function $\chi_c [p(\theta)]$. Consequently, the optimum glancing angles of the incident radiation for an observation of anomalous scattering are

$$\delta\theta/\theta_c \ll (\theta_0 - \theta_c)/\theta_c \sim 1/\mu_c, \quad (11)$$

where $\delta\theta$ is the angular resolution of the experiment.

3. Absorption of the incident radiation in the material ($\text{Im } \epsilon \neq 0$) leads to smoothing of the function $T(\theta)$ and thus a decrease in the height of the anomalous-scattering peak. If the absorption is sufficiently strong, this peak will disappear entirely (Fig. 6). The anomalous-scattering effect can thus be observed only under the condition

$$\text{Im } \epsilon \ll \text{Re } (1 - \epsilon). \quad (12)$$

The angular position of the anomalous-scattering peak depends only weakly on the absorption.

The simple model of a surface which was presented above thus successfully explains the anomalous scattering of x radiation. If this effect is to be observed experimentally, it will be necessary to satisfy conditions (10)–(12). It can be seen from Fig. 5 that the shape of the anomalous-scattering peak is described well by expression (6). At the same time, the theory predicts excessively high values for the intensity

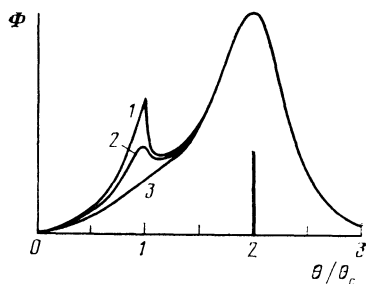


FIG. 6. Shape of the scattering function versus the absorption in the material: 1— $\text{Im } \epsilon / \text{Re } (1 - \epsilon) = 0$; 2—0.1; 3—0.5. Here the parameter value $\mu_c = 0.5$ has been used. The position of the specularly reflected beam is shown by the vertical line.

of the scattered radiation outside the region of total external reflection ($\theta > \theta_c$). A better agreement with experimental data could apparently be achieved by switching to a more elaborate model of the surface, e.g., one which incorporates the gradual, rather than abrupt, change in the electron density at the interface.^{20,22–24}

III. INTEGRAL INTENSITY OF THE SCATTERED RADIATION

Using expressions (1) and (6), we can write the integral intensity of the scattered radiation, I , as follows

$$\begin{aligned} \frac{I}{I_0} = & \frac{4k^2 R(\theta_0) \sin^3 \theta_0}{(2\pi)^{1/2} T(\theta_0)} \left[\int_0^{k \cos \theta_0} \chi_c(p) \frac{T(\theta_>)}{\sin \theta_>} dp \right. \\ & \left. + \int_0^{k(1 - \cos \theta_0)} \chi_c(p) \frac{T(\theta_<)}{\sin \theta_<} dp \right], \quad \theta_> = \arccos(\cos \theta_0 - p/k), \\ & \theta_< = \arccos(\cos \theta_0 + p/k), \end{aligned} \quad (13)$$

where the function $T(\theta)$ is given by (2). We again consider three limiting cases in terms of the values of the parameters μ and μ_c , which were introduced in (7).

1. The correlation radii are large, and the glancing angles θ_0 of the incident radiation are not too small: $\mu \gg 1$ and $\mu_c \gg 1$. As was shown above, these conditions mean that the width of the scattering function is determined exclusively by the angular width of the function $\chi_c [p(\theta)]$, which is furthermore considerably smaller than the typical change in the function $T(\theta)$. In a first approximation, we can thus set the angles $\theta_>$ and $\theta_<$ equal to θ_0 in integrals (13), and we can move the upper limits of the integration off to infinity. We then find the following well-known expression for the integral intensity of the scattered radiation:

$$I/I_0 \approx 4k^2 \xi^2 R(\theta_0) \sin^2 \theta_0, \quad \mu_c \gg 1, \quad \mu \gg 1. \quad (14)$$

This is the expression which is used in the total-integral-scattering method^{16,17} (see the Introduction).

2. The correlation radii are large, and the glancing angles of the incident radiation are extremely small: $\mu_c \gg 1$ but $\mu \ll 1$. In this case we set the angle θ_0 equal to zero in the integrals (13). To within terms on the order of θ_0^2 , the integral scattering intensity is then given by

$$\frac{I}{I_0} \approx \frac{4k^2 \theta_0}{(2\pi)^{1/2}} \int_0^k dp \chi_c(p) \left[\frac{p}{k} \left(2 - \frac{p}{k} \right) \right]^{1/2}, \quad \mu_c \gg 1, \quad \mu \ll 1. \quad (15)$$

At extremely small glancing angles of the incident radiation, the integral scattering is thus proportional to the first power of θ_0 , rather than θ_0^2 , as in the usual case, (14). This result means, in particular, that if we determine the surface-roughness height ξ from experimental data with the help of (14) then at extremely small glancing angles θ_0 the value of ξ will depend on θ_0 and will increase as this angle decreases. This apparent increase in the surface-roughness height at small values of θ_0 , which is evidence that expression (14) is not valid in this region of glancing angles, was observed in Refs. 11 and 12 and also, apparently, in Refs. 25 and 26. The effect was not explained in those papers, however.

Yet another distinctive feature of the integral scattering at small values of θ_0 is that the scattering intensity depends

on not only the roughness height ζ but also the correlation radius of the roughness, a . We will content ourselves with a qualitative discussion of this point. (Exact expressions for an exponential correlation function were derived in Ref. 21.) Let us assume that the functions $\chi(\rho)$ and $\chi_c(p)$ fall off monotonically as their arguments ρ and p increase. We denote by a the typical range of the function $\chi(\rho)$ (the correlation radius), and we assume that the typical range of $\chi_c(p)$ is a^{-1} . Using (6), we find the qualitative results

$$\begin{aligned} \chi_c(0) &\propto \zeta^2 a, \\ \int_0^k dp \chi_c(p) \left[\frac{p}{k} \left(2 - \frac{p}{k} \right) \right]^{1/2} &\approx \int_0^k dp \left(\frac{2p}{k} \right)^{1/2} \chi_c(p) \sim \frac{\zeta^2}{(ka)^{1/2}}, \\ \int_0^k dp \frac{\chi_c(p)}{\left[\frac{p}{k} \left(2 - \frac{p}{k} \right) \right]^{1/2}} &\approx \int_0^k dp \left(\frac{k}{2p} \right)^{1/2} \chi_c(p) \sim \zeta^2 (ka)^{1/2}. \end{aligned} \quad (16)$$

Using (16), we find from (15) an expression for the integrated scattering intensity as a function of the correlation radius:

$$\frac{I}{I_0} \propto \frac{k^2 \zeta^2}{(ka)^{1/2}} \theta_0, \quad \mu_c \gg 1, \quad \mu \ll 1. \quad (17)$$

3. The correlation radii are small: $\mu_c \ll 1$ and $\mu \ll 1$. In this case we can ignore the second integral in (13), and in the first we can set the function $T(\theta)$ equal to its asymptotic value (unity), since the angular width of the function $\chi_c(p)$ is considerably greater than that interval of the angle θ (from 0 to θ_c) in which the change in the function $T(\theta)$ is significant. We then have

$$\frac{I}{I_0} \approx \frac{4k^2 R(\theta_0) \sin^3 \theta_0}{(2\pi)^{1/2} T(\theta_0)} \int_0^k dp \frac{\chi_c(p)}{\left[\frac{p}{k} \left(2 - \frac{p}{k} \right) \right]^{1/2}}, \quad \mu \ll 1, \quad \mu_c \ll 1. \quad (18)$$

Using (16), we can also find an expression for the integral scattering intensity as a function of the correlation radius:

$$\frac{I}{I_0} \propto k^2 \zeta^2 (ka)^{1/2} \frac{\sin^3 \theta_0}{T(\theta_0)} R(\theta_0), \quad \mu \ll 1, \quad \mu_c \ll 1. \quad (19)$$

Let us examine this expression at glancing angles θ_0 smaller than and larger than the critical angle θ_c . In the former case ($\theta_0 < \theta_c$) the integral scattering is proportional to the first power of the glancing angle θ_0 , as in (15) and (17):

$$I/I_0 \propto k^2 \zeta^2 (ka)^{1/2} |1 - \varepsilon| \theta_0, \quad \mu < \mu_c \ll 1. \quad (20)$$

The dependence on the correlation radius in (20) is the opposite of that in (17). If the angle θ_0 instead lies outside the region of total external reflection ($\theta_0 \gg \theta_c$), we have

$$I/I_0 \propto k^2 \zeta^2 (ka)^{1/2} |1 - \varepsilon|^{2/\theta_0}, \quad \mu_c \ll \mu \ll 1. \quad (21)$$

Expressions (17) and (19)–(21) should be regarded as qualitative functional dependences. Exact relations can be found from (15) and (18) if the explicit expression for the correlation function is known. In particular, the case of an exponential correlation function was studied in Ref. 21.

CONCLUSION

1. The scattering function for the scattering of x radiation by a surface which has only a slight roughness generally has a complicated shape, which depends on both the correlation function of the surface and the optical constants of the material. It can be described on the basis of the Andronov-Leontovich theory.

2. The shape of the scattering function can conveniently be classified on the basis of the magnitude of the parameters $\mu = \pi a \theta_0^2 / \lambda$ and $\mu_c = \pi a \theta_c^2 / \lambda$, where a is the correlation radius, λ and θ_0 are the wavelength and glancing angle of the incident radiation, and θ_c is the critical angle for total external reflection. The most interesting cases are the following:

- The case $\mu \gg 1, \mu_c \gg 1$ corresponds to the usual situation in visible-range optics.
- The case $\mu_c \ll \mu \ll 1$ is characterized by an asymmetry of the scattering function and by a shift of the maximum of the scattered radiation away from the direction of specular reflection and away from the surface.
- The case $\mu_c < \mu \lesssim 1$ corresponds to the Yoneda effect.
- The case $\mu < \mu_c \ll 1$ is characterized by a weak dependence of the shape of the scattering function on the glancing angle θ_0 and by a coincidence of the maximum of the scattered radiation with the critical angle θ_c .

3. Figure 2 shows typical shapes of the scattering function. Despite the fairly general assumptions regarding the properties of the interface, however, these typical shapes do not exhaust the entire list of possible cases which can be observed experimentally. In particular, there is a discrepancy between the measured and calculated scattering intensities in the wing of the function in Fig. 5, and Fig. 2 fails to explain the results of Ref. 27, where the scattering function was observed to have a multipeak structure at scattering angles smaller than the specular angle.²⁷ It would apparently be possible to find a quantitative description of these effects either by going beyond the Andronov-Leontovich model (e.g., by using a smooth interface^{22–24}) or by considering a more complicated correlation function.

4. The dependence of the integral scattering intensity on the glancing angle of the incident beam changes in nature as we move from large glancing angles ($\mu \gg 1$) to small ones ($\mu < 1$). This change explains the experimental results of Refs. 11–13 and also makes it possible to establish a range of applicability for the total-integral-scattering method in measuring roughness height.²⁸

We wish to thank L. A. Vaĩnshteĩn, V. I. Mikerov, V. A. Slemzin, L. A. Smirnov, V. I. Tatarskiĩ, I. L. Fabelinskiĩ, and I. G. Yakushkin for a discussion of this work.

¹⁾ Andreev²⁰ was the first to call attention to the possibility of describing the Yoneda effect by perturbation theory for scattering by slightly rough surfaces.

²⁾ In that study, the interface was bombarded beforehand by high-energy heavy ions. For this reason, Petrashen' *et al.*²⁷ quite naturally link the complex nature of the scattering function not with a surface roughness but with structural changes in a surface layer.

³⁾ L. I. Mandelstam, *Ann. Phys.* **41**, 609 (1913); L. I. Mandel'shtam, *Poľnoe sobranie trudov (Complete Collected Works)*, Vol. 1, Izd. Akad. Nauk SSSR, Moscow, 1948, p. 246.

⁴⁾ A. A. Andronov and M. A. Leontovich, *Z. Phys.* **38**, 485 (1926); A. A. Andronov, *Sobranie trudov (Collected works)*, Izd. Akad. Nauk SSSR, 1955, p. 5.

- ³E. L. Feinberg, *Rasprostranenie radiovoln vdol' zemnoi poverkhnosti (Radio Wave Propagation along the Earth's Surface)*, Izd. Akad. Nauk SSSR, Moscow, 1961.
- ⁴D. E. Barrick, *Radar Cross Section Book*, Plenum Press, New York, 1970.
- ⁵A. Steyerl, *Z. Phys.* **254**, 169 (1972).
- ⁶M. A. Leontovich, *Z. Phys.* **46**, 739 (1928).
- ⁷P. P. Beckman and A. Spizzichino, *The Scattering of Electromagnetic Waves by Rough Surfaces*, Pergamon Press, New York, 1963.
- ⁸H. Reither, in: *Poverkhnostnye polyaritony (Surface polaritons)* (ed. V. M. Agranovich and A. A. Maradudin), Nauka, Moscow, 1985, p. 227.
- ⁹F. G. Bass and I. M. Fuks, *Rasseyaniye voln na statisticheski nerovnoi poverkhnosti (Wave Scattering by a Statistically Irregular Surface)*, Nauka, Moscow, 1972.
- ¹⁰M. A. Isakovich, *Obshchaya akustika (General Acoustics)*, Nauka, Moscow, 1973.
- ¹¹G. Hasinger, Preprint MPI-PAE/Extraterr. No. 163, 1980.
- ¹²B. Aschenbach, H. Bräuninger, J. Hasinger, and J. Trümper, *Proc. Soc. Phot.-Opt. Instr. Eng.* **257**, 223 (1980).
- ¹³Y. Yoneda, *Phys. Rev.* **131**, 2010 (1963).
- ¹⁴B. M. Rovinskii, V. M. Sinaiskii, and V. I. Sidenko, *Fiz. Tverd. Tela (Leningrad)* **14**, 409 (1972) [*Sov. Phys. Solid State* **14**, 340 (1972)].
- ¹⁵K. V. Kiseleva and A. G. Tur'yanskii, Preprint No. 34, P. N. Lebedev Physics Institute, Academy of Sciences of the USSR, Moscow, 1979; A. G. Tur'yanskii, Candidates's Dissertation [in Russian], FIAN SSSR, Moscow, 1980.
- ¹⁶J. M. Elson, J. P. Rahn, and J. M. Bennet, *Appl. Opt.* **22**, 3207 (1983).
- ¹⁷S. M. Rytov, Yu. A. Kravtsov, and V. I. Tatarskii, *Vvedenie v statisticheskuyu radiofiziku*, Nauka, Moscow, 1978 (*Introduction to Statistical Radiophysics*, Part II. Random Fields), Springer, New York, 1987.
- ¹⁸A. A. Maradudin and D. L. Mills, *Phys. Rev.* **B11**, 1392 (1975).
- ¹⁹A. V. Vinogradov, N. N. Zorev, I. V. Kozhevnikov, and I. G. Yakushkin, *Zh. Eksp. Teor. Fiz.* **89**, 2124 (1985) [*Sov. Phys. JETP* **62**, 1225 (1985)].
- ²⁰A. V. Andreev, *Usp. Fiz. Nauk* **145** 113 (1985) [*Sov. Phys. Usp.* **28**, 70 (1985)].
- ²¹A. V. Vinogradov, N. N. Zorev, I. V. Kozhevnikov, *et al.*, Preprint No. 319, P. N. Lebedev Physics Institute, Academy of Sciences of the USSR, Moscow, 1986.
- ²²L. A. Smirnov, T. D. Sotnikova, and Yu. I. Kogan, *Opt. Spektrosk.* **58**, 400 (1985) [*Opt. Spectrosc. (USSR)* **58**, 239 (1985)].
- ²³A. V. Andreev, *Opt. Spektrosk.* **58**, 1085 (1985) [*Opt. Spectrosc. (USSR)* **58**, 663 (1985)].
- ²⁴I. A. Artyukov and I. V. Kozhevnikov, Preprint No. 190, P. N. Lebedev Physics Institute, Academy of Sciences of the USSR, Moscow, 1988.
- ²⁵M. V. Zombeck, H. Bräuninger, A. Ondrusch, and P. Predehl, *Proc. Soc. Phot.-Opt. Instr. Eng.* **316**, 174 (1981).
- ²⁶J. R. H. Herring, *Appl. Opt.* **23**, 1156 (1984).
- ²⁷P. V. Petrashen', E. K. Kov'ev, F. N. Chukhovskii, and Yu. L. Degtyarev, *Fiz. Tverd. Tela (Leningrad)* **25**, 1211 (1983) [*Sov. Phys. Solid State* **25**, 695 (1983)].
- ²⁸I. A. Brytov and A. Ya. Grudskii, *Izmereniya, Kontrol', Avtomatizatsiya*, No. 4, 3 (1983).

Translated by Dave Parsons